To cite this article: LIU W Q, ZHANG Y Q, XIA T Y, et al. Numerical simulation of structural collapse of container ship in waves based on two-way coupling of CFD nonlinear FEM [J/OL]. Chinese Journal of Ship Research, 2023, 18(6). http://www.ship-research.com/en/article/doi/10.19693/j.issn.1673-3185.03028 (in both Chinese and English).

DOI: 10.19693/j.issn.1673-3185. 03028

Numerical simulation of structural collapse of container ship in waves based on two-way coupled CFD and nonlinear FEA

LIU Weiqin[1], *ZHANG Yaqiang*[1], *XIA Tianyu*[1], *LU Ye*[2], *YANG Meng*[3], *WU Weiguo*[4], *SONG Xuemin*[1]

1 School of Naval Architecture, Ocean and Energy Power Engineering, Wuhan University of Technology, Wuhan 430063, China
2 China Ship Scientific Research Center, Wuxi 214082, China
3 China Ship Research and Design Center, Wuhan 430064, China
4 Green & Smart River-Sea-Going Ship, Cruise and Yacht Research Center, Wuhan University of Technology, Wuhan 430063, China

Abstract: [**Objective**] The study aims to investigate the structural responses and dynamic structural collapse mode of a container ship under waves, considering the effects of load nonlinearity and surface nonlinearity. [**Methods**] First, a hydrodynamic model of the ship was established based on the CFD platform, and the overlapping mesh method was used to realize matching between the dynamic boundary mesh of the hull hydrodynamic model and the Eulerian mesh of the far-field fluid domain. The fluid volume method was used to simulate the nonlinearity of the free surface throughout the fluid domain, and the 3D N−S equations were solved in the whole fluid field domain to obtain real-time solutions of the nonlinear wave loads. Then, a nonlinear finite element analysis (FEA) model of the ship that can simulate ship hull collapse behavior was established, and the time-domain collapse response of the ship including plasticity and buckling was calculated based on the explicit dynamic nonlinear FEA method. Finally, the transmission of fluid pressure and node displacement between the hydrodynamic model and structural FEA model on the wet surface was realized. This enabled two-way iterative coupling between the CFD solver and the nonlinear FEA solver, allowing real-time calculation of the nonlinear wave loads and structural collapse responses during the structural collapse of the 4 600 TEU container ship. [**Results**] The results show that under extreme waves, the upper to middle structures of the container ship were widely plastic. The main deck, side plate, deck longitudinal, side longitudinal, and other components exhibited typical yielding and instability under waves. The deck longitudinal, side longitudinal, and other structural frames experienced serious lateral instability, and the hull structure lost its bearing capacity. [**Conclusion**] The proposed method can accurately solve the structural response and dynamic collapse mode, making it a new approach to studying the collapse response of ship structures.

Key words: structural collapse; two-way coupling; nonlinear FEA; wave loads; numerical simulation

CLC number: U663.2; U661.4

0 Introduction

Large ocean-going container ships with a large open structure and relatively low stiffness often face the risk of encountering extreme waves that surpass their ultimate bearing capacity when sailing

Received: 2022 − 08 − 08 **Accepted**: 2022 − 10 − 18

Supported by: National Natural Science Foundation of China (No. 52071243); National Defense Basic Research Program (No. JCKY202020206B037)

Authors: LIU Weiqin, born in 1985, male, Ph.D., associate professor. Research interests: the load and response of marine equipment. E-mail: liuweiqin_123@sina.com

ZHANG Yaqiang, born in 1997, male, master's degree candidate. Research interests: hydroelasticity and plasticity. E-mail: 330348703@qq.com

SONG Xuemin, born in 1986, female, Ph.D., lecturer. Research interests: computational fluid dynamics. E-mail:627500706@qq.com

***Corresponding author**: SONG Xuemin

on deep-sea routes, leading to structural collapse and breakage, thus resulting in huge loss of life and property. Between 1969 and 1994, there were 22 marine accidents worldwide caused by extreme sea conditions, resulting in the loss of over 542 lives [1]. In recent years, ship breaking accidents resulting from waves continue to occur from time to time, such as the hull breaking accident of the Japanese container ship "Comfort" in 2013 [2] and the breaking accident of the Ukrainian cargo ship "Arvin" in Turkish waters in 2021. Therefore, to prevent ship structural collapse accidents, it is necessary to accurately evaluate the structural dynamic response and collapse modes of container ships under nonlinear wave loads such as substantial deformations of the object surface, deck wetness, and slamming. Furthermore, both domestic and international ship researchers have identified this strong nonlinear fluid-solid interaction (FSI) problem as a research hotspot.

In the initial stages, solvers grounded in potential flow theory to compute wave loads were integrated with structural nonlinear solvers in academia. This implementation follows a two-step approach, where the structural collapse response of a ship is calculated by mapping the wave loads unidirectionally to the flow structure model. Masaoka [3] introduced a numerical method that integrates nonlinear finite element analysis (FEA) and the Ursell-Tasai method. This approach takes into account the nonlinear fluid forces acting on ship hull sections and computes the nonlinear bending moment on the hull's nonlinear beams. Iijima [4] introduced the concept of hydroelasticity, known as the hydroelastic method, which integrates the strip theory with the theory of nonlinear beams. This method involves numerically simulating a hydroelastic test designed to calculate the substantial deformation of the amidships corner. Liu[5] employed nonlinear strip theory to determine the maximum slamming load on the bow of a container ship when subjected to abnormal waves. This approach involves adding the calculated slamming load to the hull beam to derive its nonlinear structural response. Liu et al. [6-7] achieved the simulation of the structural collapse response of any 3D ship by integrating the 3D panel method solver with the nonlinear FEA solver. The comparison results with hydroelastic buckling test outcomes demonstrated favorable agreement. Additionally, they conducted a joint simulation using the panel method based on 3D potential flow theory and the nonlinear FEA to replicate the structural collapse response of a container ship under wave conditions.

In recent years, scholars have integrated the viscous flow theory computational fluid dynamics (CFD) solver with the FEA solver to establish a two-way FSI approach for ship structural response calculations. Takami [8] employed the CFD−FEA method to compute both the overall and local elastic responses of a ship hull structure in waves. The calculated results were then compared with those obtained through the nonlinear strip method, the panel method, and the model test results. Chen [9] analyzed hull responses under slamming load using STAR-CCM+ and ABAQUS. Jiao et al. [10] numerically investigated deck wetness and slamming of the S-175 container ship utilizing STAR-CCM+ and ABAQUS. Liu et al. [11] examined the near-shore structural hydroelasticity at model scales by employing STAR-CCM+ and ABAQUS with one-way and two-way coupling methods. Their findings indicate that the two-way coupling results demonstrate greater consistency and accuracy compared to the one-way coupling results, specifically in comparison with experimental data. At present, the two-way coupled CFD-linear FEA method is predominantly employed in studying the hydroelasticity of ship structures and has not yet been extensively utilized for investigating nonlinear issues in actual ship structures. Therefore, there is potential to incorporate the nonlinear FEA solver and the CFD solver to establish a two-way FSI approach, realizing the simulation of the structural collapse of real ships under wave conditions.

The two-step approach grounded in potential flow theory is limited to one-way coupling. This approach falls short of fully accounting for fluid viscosity and nonlinear wave loads such as free surface breaking, deck wetness, and slamming. Additionally, it fails to consider the impact of dynamic large deformation on wave loads, making it inadequate for a comprehensive assessment of ship structural collapse under wave conditions. Therefore, this paper used a two-way coupling method with a CFD solver and an explicit dynamic nonlinear FEA solver to numerically simulate the elastic, elastoplastic, and post-ultimate strength conditions of a 4 600 TEU container ship facing head-on regular waves. The objective is to analyze both the elastoplastic response and the dynamic structural collapse mode of the vessel.

1 Basic theory and numerical method

This paper employed a two-way coupling method to address the structural collapse response of the container ship under wave conditions, based on the CFD theory and explicit dynamic nonlinear FEA theory. The subsequent sections will sequentially introduce the numerical theories and methodological approaches associated with CFD, explicit dynamic nonlinear FEA, and two-way FSI.

1.1 CFD methods

The CFD solver is based on the finite volume method to solve the Navier−Stokes (N−S) equations. It partitions the flow field into control volumes of varying sizes, and the fluid flow within these control volumes is governed by the continuity and momentum equations. To balance computational accuracy and cost, the Reynolds-averaged Navier−Stokes equation (RANS) was employed. RANS decomposes velocity and pressure into instantaneous fluctuating values and average values, as illustrated in Eq. (1).

$$\frac{\partial \bar{\boldsymbol{u}}_i}{\partial t}+\bar{u}_j\frac{\partial \bar{\boldsymbol{u}}_i}{\partial \boldsymbol{x}_j}=-\frac{1}{\rho}\frac{\partial \bar{p}}{\partial \boldsymbol{x}_i}+\frac{1}{\rho}\frac{\partial}{\partial \boldsymbol{x}_j}\left(\mu\frac{\partial \bar{\boldsymbol{u}}_i}{\partial \boldsymbol{x}_j}-\rho\boldsymbol{u}_i'\boldsymbol{u}'\right) \quad (1)$$

where $\bar{\boldsymbol{u}}_i$ and $\bar{\boldsymbol{u}}_j=(\bar{u},\bar{v},\bar{w})$ are the Reynolds average velocity components in the x, y, and z directions in the Cartesian coordinate system; $\boldsymbol{x}_i$ and $\boldsymbol{x}_j=(x, y, z)$ are Cartesian coordinate values; t is time; ρ is the fluid density; $\bar{p}$ is the time-averaged pressure; μ is the dynamic viscosity coefficient of the fluid; and $\rho\boldsymbol{u}_i'\boldsymbol{u}_j'$ is the Reynolds stress term, which is a second-order tensor.

With the introduction of the Reynolds stress term to represent turbulent fluctuations, a turbulence model was applied to close the equations. In this paper, the SST k−ω turbulence model was implemented with the RANS equations to solve the entire fluid domain. Additionally, the volume of fluid (VOF) method was employed to accurately capture the free liquid surface. The transport equations for the turbulent kinetic energy and dissipation rate of the SST k−ω model are described as follows:

$$\frac{\partial}{\partial t}(\rho k)+\frac{\partial}{\partial \boldsymbol{x}_i}(\rho k u_i)=\frac{\partial}{\partial \boldsymbol{x}_j}\left(\left(\mu+\frac{\mu_t}{\sigma_k}\right)\frac{\partial k}{\partial \boldsymbol{x}_j}\right)+\tilde{G}_k-Y_k+S_k \quad (2)$$

$$\frac{\partial}{\partial t}(\rho\omega)+\frac{\partial}{\partial x_i}(\rho\omega\boldsymbol{u}_i)=\frac{\partial}{\partial \boldsymbol{x}_j}\left(\left(\mu+\frac{\mu_t}{\sigma_\omega}\right)\frac{\partial \omega}{\partial \boldsymbol{x}_j}\right)+G_\omega-Y_\omega+D_\omega+S_\omega \quad (3)$$

where k is the turbulent kinetic energy; $\tilde{G}_k$ is the generating term of turbulent kinetic energy; μ_t is the turbulent viscosity; ω is the turbulent dissipation rate; G_ω is the generating term of the specific dissipation rate; D_ω is the cross-diffusion term of ω; Y_k is the turbulent kinetic energy dissipation term of k; Y_ω is the turbulent kinetic energy dissipation term of ω; S_k and S_ω are the customized source terms; σ_k is the Prandtl number of k; σ_ω is the Prandtl number of ω.

1.2 Explicit dynamic nonlinear FEA

The generalized kinematic equation for the structural system is as follows:

$$\boldsymbol{M}\ddot{\boldsymbol{u}}+\boldsymbol{C}\dot{\boldsymbol{u}}+\boldsymbol{K}\boldsymbol{u}=\boldsymbol{P} \quad (4)$$

where $\boldsymbol{M}$, $\boldsymbol{C}$, and $\boldsymbol{K}$ are the mass matrix, damping matrix, and stiffness matrix of the object, respectively; $\boldsymbol{P}$ is the external load; $\boldsymbol{u}$, $\dot{\boldsymbol{u}}$ and $\ddot{\boldsymbol{u}}$ are the displacement, velocity, and acceleration of the object at a certain time, respectively.

This paper employed an explicit method to address the dynamic nonlinear response of the hull structure. The explicit dynamic nonlinear FEA program resolves the dynamic equilibrium equations at the onset of an incremental step. This is represented by multiplying the node mass matrix ($\boldsymbol{M}$) by the node acceleration, which is the disparity between the external force ($\boldsymbol{P}$) applied at the node and the internal force within cell ($\boldsymbol{I}$), as illustrated in Eq. (5).

$$\boldsymbol{M}\ddot{\boldsymbol{u}}=\boldsymbol{P}-\boldsymbol{I} \quad (5)$$

The acceleration is computed at time t at the start of the current incremental step:

$$\ddot{\boldsymbol{u}}|_{(t)}=(\boldsymbol{M})^{-1}\cdot(\boldsymbol{P}-\boldsymbol{I})|_{(t)} \quad (6)$$

Following this, the acceleration was temporally integrated using the central difference method. During the calculation of velocity changes, it was assumed that acceleration remained constant. The velocity and displacement were then solely dependent on the acceleration and displacement from the previous moment. This approach allows for the continuous advancement of velocity and displacement in an "explicit" manner over time, thereby completing the solution to the kinematic equations.

1.3 Two-way FSI approach

The collapse of a structure under waves involves both structural nonlinearities and wave load nonlinearities, constituting a highly nonlinear FSI problem. Addressing such an issue necessitates

multiple exchanges of physical quantities within a coupling iteration time step to obtain accurate calculation results. In this paper, a two-way implicit coupling simulation was achieved by utilizing the co-simulation functionality between the CFD platform STAR-CCM+ and the large-scale nonlinear FEA platform ABAQUS. This involved exchanging pressure and nodal displacement data at the FSI interface. From the coupling process shown in Fig. 1, it can be observed that during each iterative time step, STAR-CCM+ and ABAQUS exchange wave loads (F), as well as structural displacements and deformations (U) multiple times. In each exchange, the hydrodynamic model's mesh is updated using mesh superposition technology and the mesh "deformation" function, obtaining a new spatial position (X) and wave load (F) for the hull. This iterative exchange process continues throughout the coupling simulation. After several coupled iterations, the wave load (F), structural displacement and deformation (U), hull surface pressure (P), and hull spatial position (X) converge. Ultimately, at the end of a coupled iteration time step, a stable structural response and flow field distribution can be achieved.

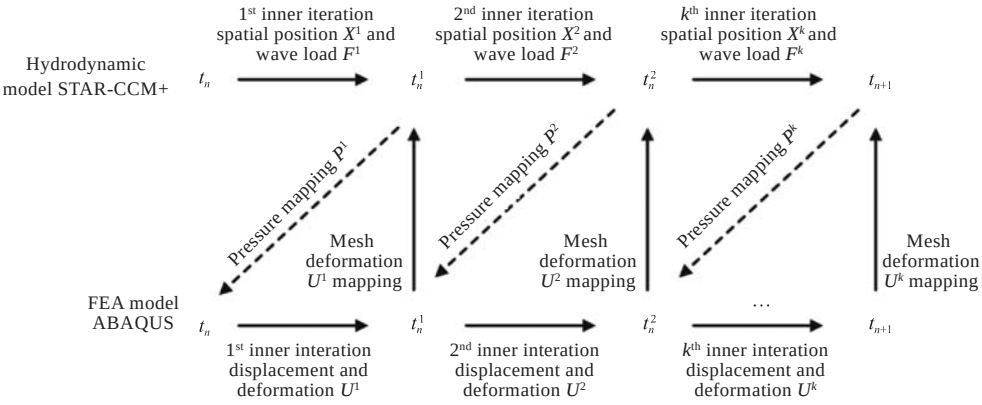

Fig. 1 Data exchange in two-way FSI within iteration time steps

Due to the need for data transfer at the FSI boundary in the FSI process, the FSI interface must adhere to the following fundamental conservation law:

$$\begin{cases} \tau_{\mathrm{f}} \times \boldsymbol{n}_{\mathrm{f}} = \tau_{\mathrm{s}} \times \boldsymbol{n}_{\mathrm{s}} \\ d_{\mathrm{f}} = d_{\mathrm{s}} \end{cases} \tag{7}$$

where τ_{f} denotes the stress in the fluid domain; τ_{s} denotes stress in the structure domain; $\boldsymbol{n}$ denotes the direction vector; d_{f} represents the displacement in the fluid domain; d_{s} represents the displacement in the structure domain.

Besides, considering the meshes of varying sizes at the FSI interface between the FEA model and the CFD model during the data transfer, the mesh interpolation challenge was addressed using the radial basis function, as depicted in the following equations:

$$\sigma(x) = \sum_{i=1}^{i=N} \alpha_i \varphi(\|x - x_i\|) + p(x) \tag{8}$$

$$\|x - x_i\| = \sqrt{(x - x_i)^2 + (y - y_i)^2 + (z - z_i)^2} \tag{9}$$

where $\sigma(x)$ is the function of x; N *is* the number of interpolation points; α_i represents the weighting coefficient to be determined; φ is the radial basis function; model $\|x-x_i\|$ is the Euclidean distance from the interpolated point x *to* x_i ; $p(x)$ is the interpolation function of the low-degree polynomial.

2 Numerical FSI modeling of 4 600 TEU container ship

A CFD hydrodynamic model and an FEA model were set up to compute the structural collapse response of a 4 600 TEU ocean-going container ship under wave conditions. This was achieved using the two-way FSI coupling CFD−FEA method. The structural configuration of the 4 600 TEU container ship incorporates a hybrid skeleton, double bottom, and double side design. The entire ship is predominantly organized with three large-opening cargo holds positioned between the wheelhouse and the forecastle. Table 1 lists the main dimensional parameters of the 4 600 TEU container ship, and Fig. 2 shows the structural geometry model.

Table 1 Main dimensions of the 4 600 TEU container ship

Parameter	Value	Parameter	Value
Length overall/m	260	Molded depth/m	19.6
Length between perpendiculars/m	247	Design draft/m	11.0
Molded breadth/m	37.3	Molded displacement volume/m^3	64 647.7

Fig. 2 Geometric model of the 4 600 TEU container ship

2.1 Hydrodynamic model

A CFD hydrodynamic model of the 4 600 TEU container ship was established, as depicted in Fig.3. The semi-implicit method, known as the Simple algorithm, was utilized to solve the pressure-coupled equation system of the N−S equations. The convection term was discretized using the upwind differencing scheme, and the $k-\varepsilon$ turbulence model was employed for turbulence flow modeling. The free surface between air and water was simulated using the VOF method. Finally, the computed wave pressure results were incorporated into the structural analysis as loads.

The computational domain encompasses both the numerical wave background domain and the overlapping region. Symmetric boundary conditions were applied to save computational costs. First, half of the wave pool background domain was generated in STAR-CCM+, with dimensions of 1 750 m in length, 500 m in width, and 750 m in height. The coordinates were set relative to the ship's length (L), approximately $-3.85L < x < 2.88L$, $0 < y < 1.92L$, and $-1.88L < z < L$. Subsequently, a half overlapping region, with dimensions of 350 m in length, 50 m in width, and 75 m in height, was established to simulate rigid body motion and facilitate fluid data transfer with the background region. The coordinates for this overlap region were defined relative to the ship's length as approximately $-0.19L < x < 1.15L$, $0 < y < 0.19L$, and $-0.096L < z < 0.19L$. The coordinate system's origin in the computational domain was positioned at the baseline of frame 0 of the ship. In this system, the x-axis points towards the bow, aligning with the ship's length; the y-axis points towards the port side, aligning with the ship's breadth; the z-axis points downward along the draft direction. The computational domain and boundaries of the 4 600 TEU container ship are illustrated in Fig. 3(a). At the overlapping mesh interface, the boundary type was set as overlapping mesh. The hull model was defined with a wall boundary type, while the symmetric section was assigned a boundary type of symmetric plane. For the inlet, starboard, and bottom boundaries, the boundary type was velocity inlet, while for the top and outlet boundaries, it was pressure outlet. Additionally, there was a wave dissipation region of 2 times the ship length at the pressure outlet boundary. This region serves to eliminate the effects of reflected waves from the wall surface and the waves induced by the hull motion on the flow field, utilizing a wave dissipation and damping method.

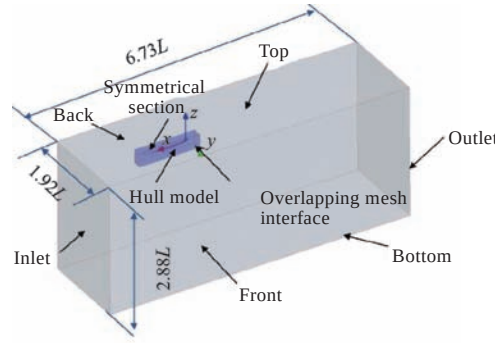

(a) Schematic of the CFD computational domain and each boundary

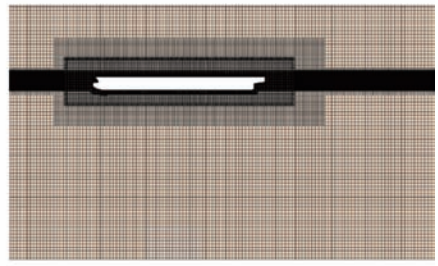

(b) Local mesh near the hull computational domain

Fig. 3 CFD hydrodynamic model of the 4 600 TEU container ship

This paper employed the cut-cell mesh generator and prism layer mesh generator to mesh the computational domain. The surface size of the hull was set at 0.5 m, similar to the mesh size of the structural finite element model, to prevent mesh interpolation errors at the FSI interface during the mapping process. A prism layer near the wall consisted of eight layers ($y+ > 300$). The maximum size of the overlapping mesh region for the hull was 1.5 m, and the maximum size of the background domain was 7.5 m. Additionally, a set of transitional meshes, with a maximum size of 4 m, was introduced between the overlapping region and the background domain. This configuration aims to mitigate flux errors resulting from the disparity between coarse and fine meshes. Finally, the free surface was divided into meshes according to the ITTC rule [12], with a minimum of 40 meshes per wavelength and at least 20 meshes per wave height. This division used a length of 1/80 of the wavelength in the wave direction and 1/20 of the wave height in the vertical direction. This ensures both the stability of the wave and the accurate capture of nonlinear

phenomena on the free surface, including liquid surface breaking, deck wetness, and slamming. The ultimate mesh configuration is depicted in Fig.3(b), comprising a total of 5.27 million cells, with 2.02 million cells in the overlapping region.

2.2 Structural nonlinear FEA model

A half FEA model of the 4 600 TEU container ship structure was constructed by integrating the pre-processing software HYPERMESH with the large-scale structural nonlinear calculation platform ABAQUS, as shown in Fig. 4. To prevent potential errors arising from the singularity of the stiffness matrix during calculations, a row of nodes was strategically selected at the stern to constrain the hull's movement along the *x*-axis. This constraint implemented is to prevent undesired drifting of the hull under the influence of waves. Symmetric boundary conditions were applied in the longitudinal section of the hull, and the specifics of these boundary conditions can be found in Table 2. The time-domain responses of the ship structure were computed using explicit dynamics nonlinear FEA. A finite element mesh size of 0.5 m was employed to ensure the alignment of the surface mesh with the hydrodynamic hull and to accurately simulate the buckling behavior of the hull. The ultimate FEA model comprises 216 485 elements.

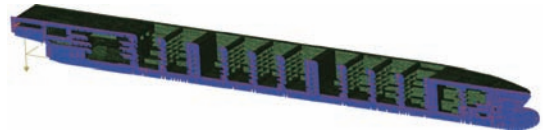

Fig. 4 FEA model of the 4 600 TEU container ship

Table 2 Boundary conditions

Position	U_x	U_y	U_z	U_{Rx}	U_{Ry}	U_{Rz}
Stern	Constrained	Unconstratined	Unconstratined	Unconstratined	Unconstratined	Unconstratined
Longitudinal section in center place	Unconstratined	Constrained	Unconstratined	Constrained	Unconstratined	Constrained

This paper primarily employed a two-way coupling method based on a viscous flow solver to investigate ship collapse issues. It specifically focuses on structural collapse problems under the nonlinear transient wet surface without greatly increasing the wave height. Additionally, to enhance the efficiency of numerical simulation, a certain degree of strength weakening treatment was applied to the plate thickness while ensuring that the stiffness distribution of the hull structure aligned with that of the actual hull structure. In this paper, the hull structure is composed of Q235 steel, and the constitutive model adopts an ideal elastoplastic material. The specific material parameters are detailed in Table 3.

Table 3 Material parameters of hull structure

Density/ ($t \cdot m^{-3}$)	Modulus of elasticity/MPa	Poisson's ratio	Yield strength/MPa	Permissible stress/MPa
7850	2.06×10^5	0.33	235	211

2.3 Coupling calculation settings

In STAR-CCM+ and ABAQUS, the outer hull surface was designated as the FSI interface. Through this interface, real-time exchange of pressure data from the flow field and displacement data from the structural response was facilitated, enabling the solution of the two-way FSI problem. Surface-to-surface mapping was chosen for data mapping. The pressure field, including the dynamic pressure in the flow field and the wall shear force, was mapped from the flow field to the hull surface of the structural solver through the FSI interface. The displacement field under the water pressure was solved in ABAQUS and transferred back to the flow field through the FSI interface; after updating the flow field, one complete two-way coupling calculation was completed. The implicit coupling algorithm was chosen, with five data exchanges per time step, and multiple internal iterations for each exchange. The fluid calculator carried out 10 internal iterations in one calculation time step. A constant coupling time step of 0.005 s was chosen. The co-simulation was performed through a server powered by an Intel Xeon E5-2660 with 20 cores and 40 threads for parallel computation. It took approximately 15 days to compute one set of conditions.

2.4 Computational conditions setup

Computational conditions were formulated to study the structural collapse response characteristics of a 4 600 TEU container ship under different wave parameters. The computational conditions are shown in Table 4. The waves involved in all conditions were first-order linear waves, with a

wavelength of one ship length (247 m). The wave height started at 2.5 m and increased to 15 m at intervals of 2.5 m, ensuring that the hull structure experienced elastic deformation, elastoplastic deformation, ultimate strength deformation, and post-ultimate strength deformation under the wave loads. In this paper, four typical nodes were selected in the collapse region amidships from the deck to the bottom of the ship, located on the main deck, the side plate, the bilge plate, and the bottom plate. These nodes were named Node 1, Node 2, Node 3, and Node 4 respectively, as shown in Fig. 5, for outputting the time-domain elastoplastic stress curves to determine if the structure collapsed.

Table 4 Numerical simulation conditions for collapse responses of overall hull

Condition	Wave length/ ship length	Wave height/m	Condition	Wave length/ ship length	Wave height/m
H_1	1	2.5	H_4	1	10.0
H_2	1	5.0	H_5	1	12.5
H_3	1	7.5	H_6	1	15.0

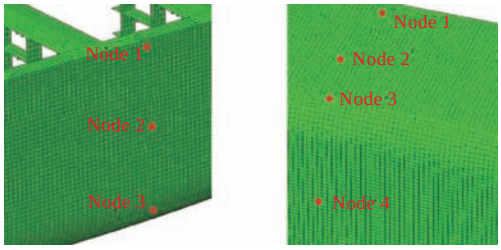

Fig. 5 Positions of typical stress nodes

3 Result analysis

3.1 CFD mesh independence verification

First, a mesh independence verification for the CFD calculation of condition H_1 was conducted. Three sets of meshes were established: a (coarse), b (medium), and c (fine), with base sizes of 12.5, 7.5, and 5 m, respectively. The number of meshes was 2.84 million, 5.27 million, and 9.98 million, respectively. The results for heave, pitch, and stress at Node 2 for the three sets of generated meshes are illustrated in Fig. 6. It can be observed that the calculation amplitudes of the coarse mesh are smaller compared to the fine mesh, with heave amplitude about 9.1% smaller, pitch amplitude about 7.6% smaller, and the stress amplitude about 7.9% smaller. The calculated amplitudes of the medium mesh and the fine mesh are very close, with deviations of the heave amplitude, pitch, and stress approximately 3.3%, 2.1%, and 2.5%, respectively. Taking into account the efficiency of numerical computation, the medium mesh was chosen for the computation.

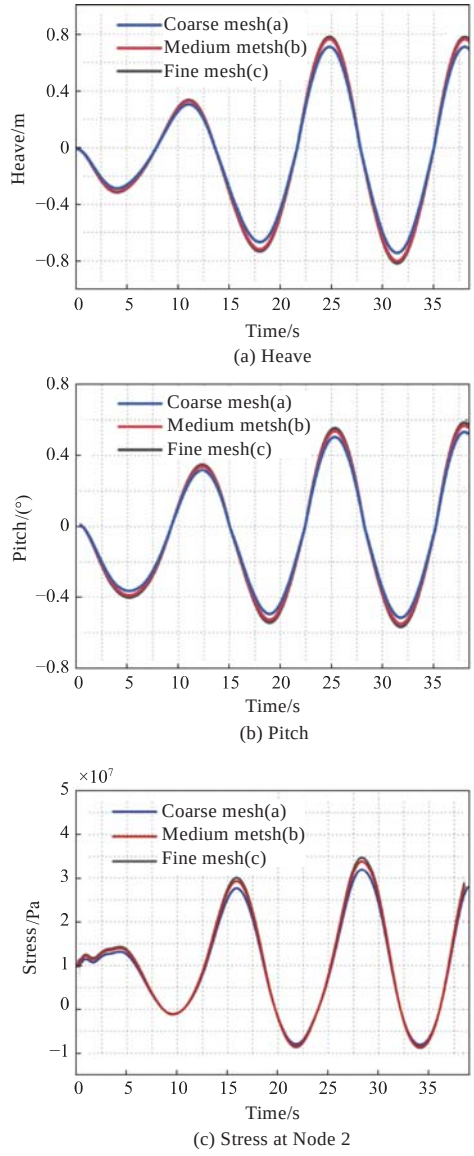

Fig. 6 Mesh independence verification

3.2 Time-domain stress curve of typical nodes

The two-way FSI coupling CFD-nonlinear FEA method, as introduced in this paper, was applied to compute the two-way FSI problem of the 4 600 TEU container ship. The elastic and elastoplastic responses of the 4 600 TEU container ship were then determined under six specified computational conditions, as illustrated in Table 4. The ultimate longitudinal stress outcomes for typical nodes along the ship's length are depicted in Fig. 7, where positive values indicate compression and negative values denote tension. The figure reveals that the overall stress curve did not exhibit a pronounced hydroelastic vibration response. This observation

can be attributed to two main factors. Firstly, wave-induced vibration typically occurs when the total first-order vibration frequency of the ship hull aligns with multiples of the wave encounter frequency. Even in cases of wave-induced vibration of container ships, such phenomena do not occur at any frequency. Secondly, in the simulations conducted in this paper, the ship remained stationary under the waves without giving it a sailing speed, resulting in a small slamming force and no significant flutter phenomenon. Additionally, the primary focus of this paper is on elastoplastic responses and collapse issues, and the selected conditions for calculation deliberately exclude scenarios that might trigger hydroelastic vibration responses.

Fig. 7(a) and Fig. 7(b) illustrate the stress curves for conditions H_1 (with a wave height of 2.5 m) and H_2 (with a wave height of 5.0 m), respectively. The figures indicate that the wave loads remained relatively small throughout the two-way coupling process. In both cases, the stress curves of typical nodes exhibited elastic responses. From Fig. 7(c) and Fig. 7(d), which depict the stress curves for conditions H_3 (with a wave height of 7.5 m) and H_4 (with a wave height of 10.0 m), respectively, it is observed that Node 1 under condition H_3 entered plasticity at 14.96 s, while Node 2 entered plasticity at 26.76 s. In condition H_4, Node 1 entered plasticity at 14.01 s, and Node 2 entered plasticity at 28.26 s. Nodes 3 and 4 did not enter plasticity in either case. This trend reveals that as wave height increases, the rate at which the ship's structure enters plasticity accelerates. Additionally, as local structures undergo plasticity,

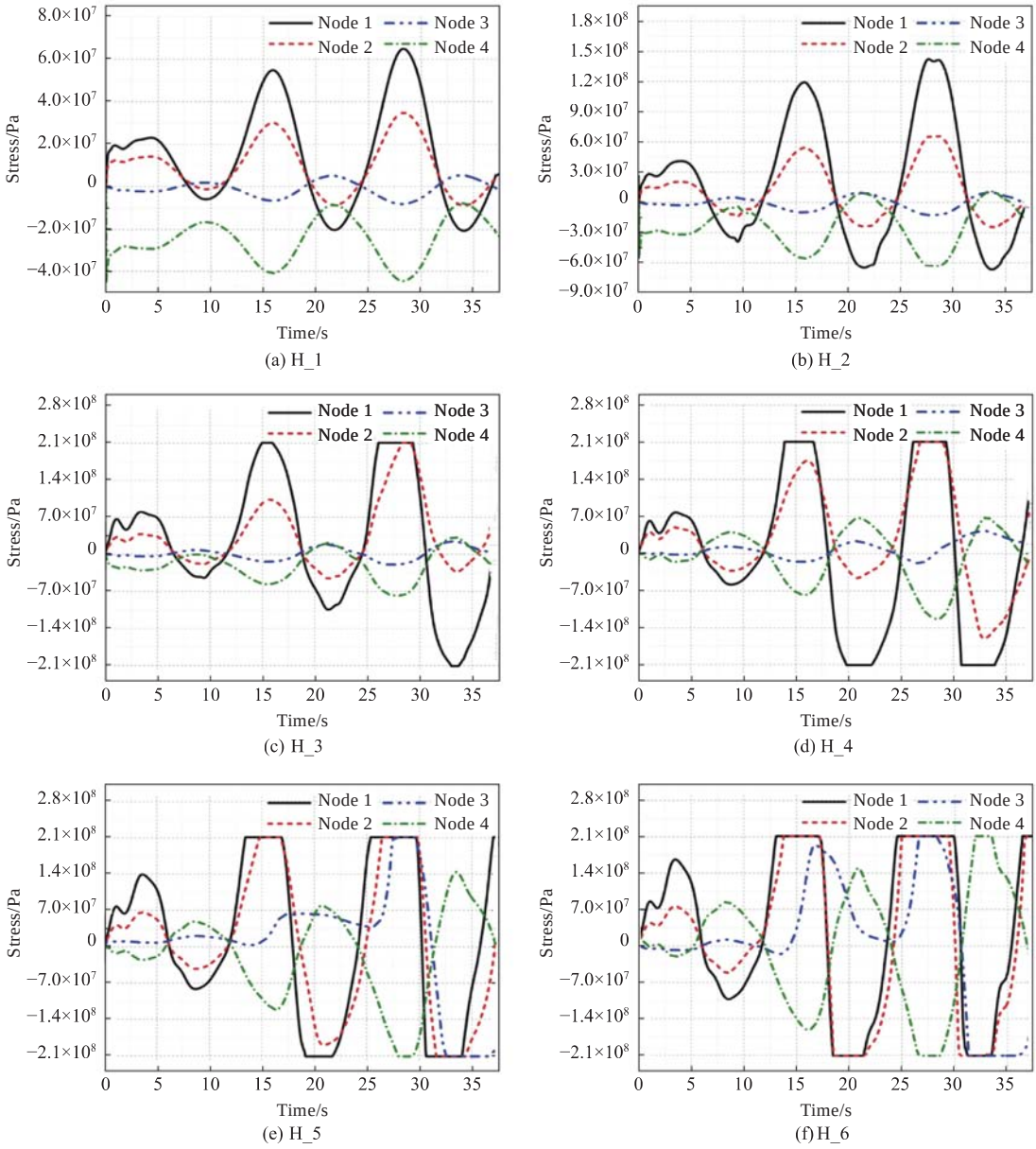

Fig. 7 Time-domain elastoplastic stress curves of typical nodes under various conditions

their stiffness diminishes, leading to a reduced capacity to withstand deformation. Consequently, sagging deformation in the mid-arch intensifies. By examining Fig. 7(e) and Fig. 7(f), which represent conditions H_5 (with a wave height of 12.5 m) and H_6 (with a wave height of 15.0 m), respectively, a heightened rate of plasticity entry in the ship structure with the increasing wave height can be observed. Besides, most nodes entered plasticity, and the structure entered a state of collapse. The stress curves began to lose periodicity and adopted an irregular shape as the collapse progressed. This is attributed to the decreasing or even loss of load-bearing capacity during the collapse and the intricate out-of-plane large deformation affecting the flow field's wave loads.

3.3 FSI collapse mode analysis under typical conditions

In the two-way FSI process, contour maps generated by the hydrodynamic and structural models allow for the visualization of the relationship between the hull structural responses, ship buoyancy, and water pressure on the hull at any given moment. Therefore, this paper chose condition H_5 as a representative case for analyzing the collapse mode considering FSI, showing its collapse mode at the sagging moment, as shown in Figs. 8−10. From Fig. 8, which depicts the wave-free surface distribution of the 4 600 TEU container ship under the typical condition H_5, it can be observed that when the wave trough was in proximity to the amidships profile, the hydrodynamic model accomplished the mesh mapping of the heave, pitch, and sagging deformations generated by the FEA model through the FSI interface, resulting in noticeable collapse deformations and trim, as well as significant bow waves impacting the deck and slamming at the stern. Fig. 9 displays the pressure distribution on the wet surface of the container ship, where dynamic waves induced a significant pressure distribution on the ship that was mapped onto the structural FEA model during the two-way coupling process. The pressure distributions of the two aligned completely, showing a successful mapping of the wave loads. From Fig.10, which presents a contour map illustrating the structural stress and deformation of the container ship, it can be observed that the upper to middle structures of the container ship entered extensive plasticity at this point. Components such as the main deck, side plates, deck longitudinals, and side longitudinals underwent deformation under wave loads, leading to noticeable yielding and buckling instability. The main deck and side plating exhibited prominent wrinkles, while the deck longitudinals, side longitudinals, and other stiffeners experienced serious lateral instability. The plastic deformation area extended from the side plate to the ship's bottom plate. This indicates that condition H_5 caused widespread structural collapse of the 4 600 TEU container ship, resulting in the complete loss of its load-bearing capacity.

Fig. 8 Wave-free surface distribution (with a wave height of 12.5 m)

Fig. 9 Contour map of wave pressure (with a wave height of 12.5 m)

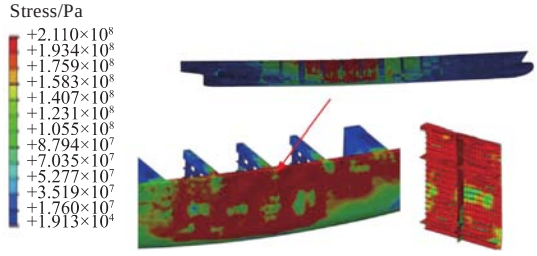

Fig. 10 Stress contours of hull structure and deformation (with a wave height of 12.5 m)

3.4 Effect of wave loads on overall and local deformation

To illustrate the correlation between the overall and local deformation responses of the hull and the magnitude of wave loads, maximum deformation values of yaw angle and typical nodal stress were extracted from the six typical conditions for comparative analysis. The outcomes are presented in Fig. 11. As evident from Fig. 11(a), the maximum yaw angle increased with the elevation of wave height. When the wave height remained below 10 m, the midship structure experienced the elastic and elastoplastic stages due to the small wave load, resulting in limited deformation of the yaw angle. However, when the wave height surpassed 10 m, the wave loads exceeded the ship's load-carrying

capacity. At this point, the midship structure underwent extensive plasticity, causing a significant reduction in carrying capacity and a rapid increase in the maximum deformation values of yaw angle, signifying an evident collapse and damage to the hull structure. From Fig. 11(b), it is evident that the stress in the local structure increased with the augmentation of wave height. The deck (Node 1) and side plate (Node 2) entered into plasticity more rapidly compared to the bilge plate (Node 3) and bottom plate (Node 4) due to their distance from the neutral axis.

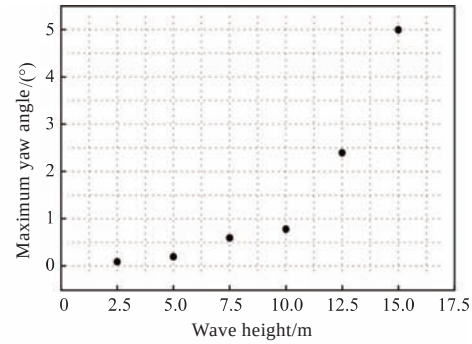

(a) Variation of maximum deformation of yaw angle with wave height

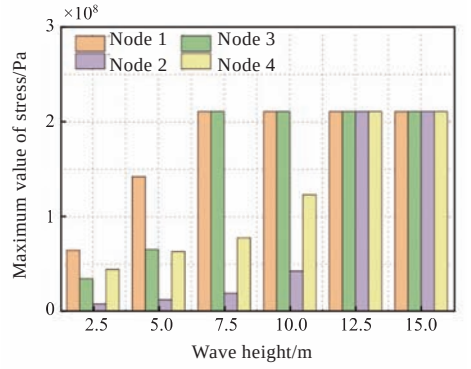

(b) Variation of maximum stress of local structure with wave height

Fig. 11 Variation of maximum local and overall deformation with wave height

4 Conclusions

The paper established a CFD hydrodynamic model and a nonlinear FEA model for the structural analysis of a 4 600 TEU container ship. Various typical wave conditions were selected, and a two-way FSI coupling CFD-nonlinear FEA method was employed to simulate the structural elastoplastic responses of the container ship. The study investigated typical nodal stress curves and FSI collapse modes. The conclusions are as follows:

1) The two-way FSI coupling CFD-nonlinear FEA method allows for the consideration of the influence of nonlinear wave loads such as deck wetness, instantaneous wet surfaces, and significant deformations of the hull. This method achieves a two-way FSI mapping of fluid loads and structural displacements and deformations, providing a new approach for accurately assessing the structural response and dynamic collapse processes of ships under waves.

2) When the wave height is relatively small, the ship's hull structure experiences linear elastic deformation or small-scale structural plastic deformation and the structure remains in a safe state. However, when the wave height exceeds a certain threshold, the vessel transitions from partial structural plasticity to extensive plasticity, leading to structural collapse. Moreover, as the wave height increases, the rate at which the structure enters plasticity accelerates.

3) The 4 600 TEU container ship, being a large open hatch vessel with the neutral axis distant from the deck area, exhibits a structural collapse mode known as midship collapse under wave conditions. This is characterized by the onset of yielding and buckling in the deck and upper hull structures. Under the influence of cumulative plastic effects, this failure gradually spreads from the ship's side plate toward the bottom plate, ultimately leading to a complete loss of load-bearing capacity and significant longitudinal deformation of the entire structure.

The study solely assessed the structural collapse response of the 4 600 TEU container ship at zero speed. Further research is needed to investigate the impact of slamming-induced vibrations and wave-induced vibrations on the collapse response under sailing conditions.

References

[1] KHARIF C, PELINOVSKY E. Physical mechanisms of the rogue wave phenomenon [J]. European Journal of Mechanics-B/Fluids, 2003, 22(6): 603−634.

[2] ANDERS M. Update on incident involving the containership MOL Comfort [J]. American Journal of Transportation, 2013, 558: 19.

[3] MASAOKA K, OKADA H. A numerical approach for ship hull girder collapse behavior in waves [C]//Proceedings of the 13th International Offshore and Polar Engineering Conference. Honolulu, Hawaii, USA: The International Society of Offshore and Polar Engineers, 2003.

[4] IIJIMA K, KIMURA K, XU W J, et al. Hydroelasto-plasticity approach to predicting the post-ultimate strength behavior of a ship's hull girder in waves [J]. Journal of Marine Science and Technology, 2011, 16 (4): 379−389.

[5] LIU W Q, SUZUKI K. Structural response study of ship beam under large slamming load [J]. Journal of the Japanese Society of Naval Architects and Ocean Engineers, 2012, 2: 509−512.

[6] LIU W Q, HUANG Y, WANG X M, et al. Numerical simulation and model experiment of structural collapse of ship in waves [J]. Navigation of China, 2021, 44(1): 21−26 (in Chinese).

[7] LIU W Q, QU H T, HUANG Y, et al. Simulation study of dynamic collapse of container ship structure under the action of wave [J]. Navigation of China, 2022, 45 (1): 43−49 (in Chinese).

[8] TAKAMI T, MATSUI S, OKA M, et al. A numerical simulation method for predicting global and local hydroelastic response of a ship based on CFD and FEA coupling [J]. Marine Structures, 2018, 59: 368−386.

[9] CHEN Y. Fluid-structure coupling response of a large ship hull under wave slamming loads based on VOF method [D]. Zhenjiang: Jiangsu University of Science and Technology, 2019 (in Chinese).

[10] JIAO J L, HUANG S X, TEZDOGAN T, et al. Slamming and green water loads on a ship sailing in regular waves predicted by a coupled CFD – FEA approach [J]. Ocean Engineering, 2021, 241: 110107.

[11] LIU W Q, LUO W P, YANG M, et al. Development of a fully coupled numerical hydroelasto-plastic approach for offshore structure [J]. Ocean Engineering, 2022, 258: 111713.

[12] ITTC. Recommended procedures and guidelines: practical guidelines for ship CFD applications [S]. [S.1.]: ITTC, 2011.

基于CFD—非线性有限元双向耦合的集装箱船波浪下结构崩溃数值仿真

刘维勤[1], 张亚强[1], 夏天禹[1], 陆晔[2], 杨萌[3], 吴卫国[4], 宋学敏[*1]

1 武汉理工大学 船海与能源动力工程学院,湖北 武汉 430063

2 中国船舶科学研究中心,江苏 无锡 214082

3 中国舰船研究设计中心,湖北 武汉 430064

4 武汉理工大学 绿色智能江海直达船舶与邮轮游艇研究中心,湖北 武汉 430063

摘　要:[**目的**]充分考虑载荷非线性和物面非线性因素的影响,研究集装箱船在波浪下结构响应及动态结构崩溃模式。[**方法**]首先,基于CFD平台建立船舶水动力模型,采用重叠网格法实现船体水动力模型动边界网格与远场流体域的欧拉网格间的匹配,在流体全域内采用流体体积法模拟自由面非线性,在流场全域内求解三维N−S方程,实时求解非线性波浪载荷;然后,建立可模拟船舯崩溃行为的船舶非线性有限元模型,基于显式动力学非线性有限元法计算包含塑性和屈曲的时域崩溃响应;最后,实现水动力模型与结构有限元模型在湿表面上的流体压力和节点位移的传递,以此进行CFD求解器与非线性有限元求解器间的双向迭代耦合,并实时计算4 600 TEU集装箱船结构崩溃过程中的非线性波浪载荷和结构崩溃响应。[**结果**]结果显示,在极端波浪下上部至中部结构广泛进入塑性状态,主甲板、舷侧板、甲板纵骨和舷侧纵骨等构件在波浪下出现明显的屈服及失稳,甲板纵骨和舷侧纵骨等骨材发生严重的侧向失稳,船体结构丧失了承载能力。[**结论**]所提方法可较准确求解结构响应及动态崩溃模式,可作为研究船舶结构崩溃响应的一种新方法。

关键词:结构崩溃;双向耦合;非线性有限元法;波浪载荷;数值仿真